

## Overview of the Neutrinos from Stored Muons Facility - nuSTORM

To cite this article: D. Adey *et al* 2017 *JINST* **12** P07020

View the [article online](#) for updates and enhancements.

### You may also like

- [Neutrino–nucleus cross sections for oscillation experiments](#)  
Teppei Katori and Marco Martini
- [Precision measurements and tau neutrino physics in a future accelerator neutrino experiment](#)  
Jian Tang, Sampsa Vihonen and Yu Xu
- [The discovery reach of CP violation in neutrino oscillation with non-standard interaction effects](#)  
Zini Rahman, Arnab Dasgupta and Rathin Adhikari



**ECS**  
The  
Electrochemical  
Society  
Advancing solid state &  
electrochemical science & technology

**DISCOVER**  
how sustainability  
intersects with  
electrochemistry & solid  
state science research

## MUON ACCELERATORS FOR PARTICLE PHYSICS — MUON

# Overview of the Neutrinos from Stored Muons Facility - nuSTORM

D. Adey,<sup>a,1</sup> R.B. Appleby,<sup>b</sup> R. Bayes,<sup>c</sup> A. Bogacz,<sup>d</sup> A.D. Bross,<sup>a,2</sup> J.-B. Lagrange,<sup>e,3</sup> A. Liu,<sup>a,4</sup>  
D. Neuffer,<sup>a</sup> J. Pasternak<sup>e,f</sup> and S. Tygier<sup>b</sup>

<sup>a</sup>Accelerator Physics Center, Fermi National Accelerator Laboratory,  
Wilson Road, Batavia, IL, U.S.A.

<sup>b</sup>Cockcroft Institute, University of Manchester,  
Oxford Road, Manchester, U.K.

<sup>c</sup>School of Physics and Astronomy, University of Glasgow  
Glasgow G12 8QQ, U.K.

<sup>d</sup>Thomas Jefferson National Laboratory  
2000 Jefferson Avenue, Newport News, Virginia, U.S.A.

<sup>e</sup>Department of Physics, Imperial College London,  
Exhibition Road, London, U.K.

<sup>f</sup>ISIS Department, Rutherford Appleton Laboratory,  
Didcot OX11 0QX, U.K.

E-mail: [bross@fnal.gov](mailto:bross@fnal.gov)

**ABSTRACT:** Neutrino beams produced from the decay of muons in a racetrack-like decay ring (the so called Neutrino Factory) provide a powerful way to study neutrino oscillation physics and, in addition, provide unique beams for neutrino interaction studies. The Neutrinos from STORED Muons (nuSTORM) facility uses a neutrino factory-like design. Due to the particular nature of nuSTORM, it can also provide an intense, very pure, muon neutrino beam from pion decay. This so-called “Neo-conventional” muon-neutrino beam from nuSTORM makes nuSTORM a hybrid neutrino factory.

In this paper we describe the facility and give a detailed description of the neutrino beams that are available and the precision to which they can be characterized. We then show its potential for a neutrino interaction physics program and present sensitivity plots that indicate how well the facility can perform for short-baseline oscillation searches. Finally, we comment on the performance potential of a “Neo-conventional” muon neutrino beam optimized for long-baseline neutrino-oscillation physics.

**KEYWORDS:** Accelerator Applications; Neutrino detectors

<sup>1</sup>Currently at the Institute for High Energy Physics, Beijing.

<sup>2</sup>Corresponding author.

<sup>3</sup>Currently at CERN, Geneva, Switzerland.

<sup>4</sup>Currently at Euclid Techlabs, 365 Remington Blvd Bolingbrook, IL.

---

## Contents

<b>1</b>	<b>Introduction</b>	<b>1</b>
<b>2</b>	<b>The nuSTORM facility</b>	<b>2</b>
<b>3</b>	<b>Facility details</b>	<b>3</b>
3.1	Decay ring	4
<b>4</b>	<b>Performance</b>	<b>6</b>
4.1	Neutrino fluxes and event samples	7
4.2	Search for light-sterile neutrinos	9
4.2.1	Far Detector	9
4.2.2	Results	9
<b>5</b>	<b>Optimization of the nuSTORM pion beam line for long-baseline oscillation physics</b>	<b>10</b>
5.1	nuPIL design based on the FFAG principle	13
<b>6</b>	<b>Conclusions</b>	<b>13</b>

---

## 1 Introduction

The nuSTORM facility has been designed to deliver beams of  $\overline{\nu}_e$  and  $\overline{\nu}_\mu$  from the decay of a stored  $\mu^\pm$  beam with a central momentum of 3.8 GeV/c [1, 2]. The facility has three primary physics objectives:

- Serve future long- and short-baseline neutrino-oscillation programs by providing definitive measurements of  $\overline{\nu}_e N$  and  $\overline{\nu}_\mu N$  scattering cross sections with percent-level precision;
- Allow searches for sterile neutrinos of exquisite sensitivity to be carried out; and
- Constitute a crucial first step in the development of muon accelerators as a powerful new technique for particle physics.

The nuSTORM facility represents the simplest implementation of the Neutrino Factory concept [3]. Protons are used to produce pions off a conventional solid target. These pions are then collected with a magnetic horn and quadrupole magnets and are transported to, and injected into, a decay ring. The pions that decay in the first straight of the ring can yield muons that are captured in the ring. The circulating muons then subsequently decay into electrons and neutrinos. A decay ring design was developed that is optimized for a 3.8 GeV/c muon central momentum. This momentum was selected to maximize the physics reach for both  $\nu$  oscillation and cross section physics. See figure 1



**Figure 1.** Schematic of the facility.

for a schematic of the facility. The nuSTORM facility can be considered a “near-term” facility, since if funds were available, it could be built without the development of any new technology.

Muon decay yields a neutrino beam of precisely known flavor content and energy. In addition, if the circulating muon flux in the ring is measured accurately (with beam-current transformers, for example), then the neutrino beam flux is also accurately known. Near and far detectors are placed along the line of one of the straight sections of the racetrack decay ring. Purpose-specific near detectors can be located in a near hall ( $\approx 50$  m from the end of the decay ring straight) and will measure neutrino-nucleon cross sections and can provide the first precision measurements of  $\nu_e$  and  $\bar{\nu}_e$  cross sections in the energy range  $1 \leq E_\nu \leq 4$  GeV. A far detector at  $\approx 2000$  m would study neutrino oscillation physics and would be capable of performing searches in both appearance and disappearance channels. The experiment will take advantage of the “golden channel” of oscillation appearance  $\nu_e \rightarrow \nu_\mu$  ( $\mu^+$  stored in the ring;  $\mu^+ \rightarrow e^+ + \nu_e + \bar{\nu}_\mu$ ), where the resulting final state has a muon of the wrong-sign from interactions of the  $\bar{\nu}_\mu$  in the beam. This detector would need to be magnetized for the wrong-sign muon appearance channel, as is the case for the current baseline Neutrino Factory detector [4]. A number of possibilities for the far detector exist. However, a magnetized iron detector similar to that used in MINOS appears to be the most straight forward and cost effective approach.

## 2 The nuSTORM facility

The components of nuSTORM consist of six major elements: the primary proton beam line, target station, pion transport line, muon decay ring, near and far detector halls [5].

At Fermilab, a candidate site for the facility was identified. It would be located south of the existing Main Injector accelerator and west of Kautz Road. The proton beam will be extracted from the Main Injector at the existing MI-40 absorber and directed east towards a new below grade target station, pion transport line and muon decay ring. The neutrino beam will be directed towards a near detector hall located  $\approx 50$  m east of the muon decay ring and towards the far detector located approximately 2 km away in the existing D0 Assembly Building (DAB). Figure 2 shows the nuSTORM facility components as they would be sited near the Main Injector. The nuSTORM facility will follow, wherever possible (primary proton beam line, target, horn, etc.), NuMI [6] designs. Our plan is to extract one “booster batch” at 120 GeV from the Main Injector ( $\approx 8 \times 10^{12}$  protons) and place this beam on a carbon target. Forward pions are focused by a horn into a capture and transport channel. Pions are then “stochastically” injected into the decay ring (see [7, 8]). Pion decays within the first straight of the decay ring can yield a muon that is stored in the ring. Muon decay within the straight sections will produce  $\nu$  beams of known flux and flavor via:  $\mu^+ \rightarrow e^+ + \bar{\nu}_\mu + \nu_e$  or  $\mu^- \rightarrow e^- + \nu_\mu + \bar{\nu}_e$ . For the implementation which is described here,

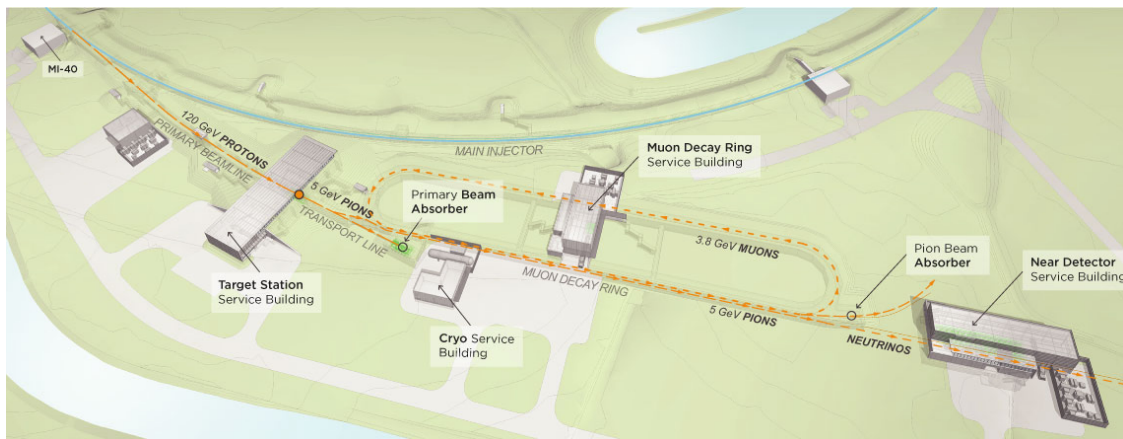


**Figure 2.** nuSTORM facility components.

we chose a 3.8 GeV/c decay ring to obtain the desired spectrum of  $\approx 2$  GeV neutrinos. This means that we capture pions at a momentum of approximately 5 GeV/c.

### 3 Facility details

As mentioned above, the primary proton beam line and target station (and its components, i.e., target and horn) for nuSTORM follow the NuMI designs. From the downstream end of the horn, however, the nuSTORM beam system is no longer similar to a conventional neutrino beam. From the downstream end of the horn, we continue the pion transport with several radiation-hard (MgO insulated) quadrupoles. Although conventional from a magnetic field point of view, the first two to four quadrupoles need special and careful treatment in their design, in order to maximize their lifetime in this high-radiation environment. The pion beam ( $5 \pm 1.0$  GeV/c) is brought out of the target station and transported to the injection point of the decay ring, which we have called the “Orbit Combination section” (OCS), where a large dispersion is introduced in order to combine the pion and muon reference orbits. Figure 3 gives a schematic of this concept. In the “production straight

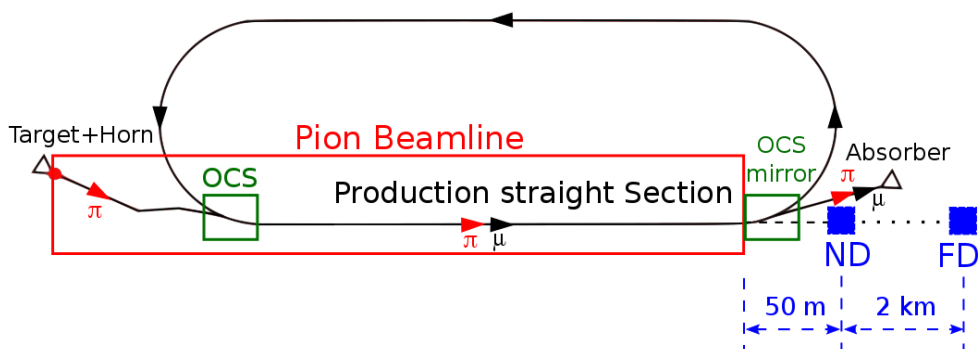


**Figure 3.** Schematic of pion injection into the nuSTORM ring.

section”, approximately 50% of the pions decay into muons, a fraction of which are captured within the ring’s acceptance. The figure-of-merit for the baseline nuSTORM design is that  $8 \times 10^{-3}$  muons are stored in the ring per proton on target (POT). The decay ring straight-section FODO cells were designed to have betatron functions  $\beta_x, \beta_y$  (the Twiss parameters) optimized for beam acceptance and neutrino beam production (small divergence relative to the muon opening angle ( $1/\gamma$ ) from  $\pi \rightarrow \mu$  decay). At the end of the production straight there is a mirror of the OCS which removes the pions that have not decayed, along with muons coming from the very forward decay of pions, and transports these particles to a beam absorber. With a beam absorber depth of  $\sim 3.5$  m, all the pions are absorbed, but the muons produce an intense, pulsed low-momentum muon beam ( $10^{10}$ /pulse with  $100 \leq P \leq 300$  MeV/c) exiting the back of the absorber.

Large betatron functions increase the beam size leading to aperture losses, while smaller betatron functions increase the divergence of the muon beam. Balancing these criteria, we have chosen FODO cells with  $\beta_{\max} \sim 30.2$  m, and  $\beta_{\min} \sim 23.3$  m for the 3.8 GeV/c muons, which for the 5.0 GeV/c pions, implies  $\sim 38.5$  m and  $\sim 31.6$  m for the pion’s  $\beta_{\max}$  and  $\beta_{\min}$ , respectively.

The nuSTORM pion beamline consists of the pion delivery section, starting from the downstream end of the horn to the OCS, followed by the production straight section of the muon decay ring (see the red enclosure in figure 3). The linear optics of the pion beamline, from the downstream end of the horn into the production straight FODO cells, are shown in figure 4. (Only one FODO cell is shown to omit the periodic Twiss values.) The design of the optics from the first dipole to the end of the production straight has been fixed to provide the best stochastic injection performance and a good accommodation of both the pion and the muon beams in the production straight [9]. The production straight contains 21 FODO cells, with a total length of  $\sim 150$  meters. The length of the pion beamline is  $\sim 200$  meters, in whose length approximately 50% of the 5 GeV/c pions will decay to muons. A large dispersion,  $D_x$ , is required at the injection point, in order to achieve  $\pi$  and  $\mu$  beam separation. The OCS readily reaches this goal. A schematic drawing of the injection scenario is shown in figure 5. The pure sector dipole for muons in the OCS has an exit angle for pions that is non-perpendicular to the edge, and the pure defocusing quadrupole in the OCS for muons is a combined-function dipole for the pions, with both entrance and exit angles non-perpendicular to the edges. The OCS will be followed by a short matching section to the decay FODO cells. The performance of the injection scenario can be gauged by determining the number of muons at the end of the decay straight using a G4beamline simulation. In this simulation, we were able to obtain 0.012 muons per POT (see figure 6). These muons have a wide momentum range, which is beyond that which the ring can accept ( $3.8$  GeV/c  $\pm 10\%$ ) and thus will only be partly accepted by the ring. The green region in figure 6 shows the  $3.8 \pm 10\%$  GeV/c acceptance of the ring, and the red region shows the high momentum muons which will be extracted by the mirror OCS at the end of the injection straight (see below). Within the acceptance of the decay ring, we obtain approximately 0.008 muons per POT.

### 3.1 Decay ring

We propose a compact (480 m in circumference) racetrack ring design based on large aperture, separate function magnets (dipoles and quadrupoles). The ring is configured with FODO cells combined with DBA (Double Bend Achromat) optics. The ring layout, including pion injection/extraction points, is illustrated in figure 7 and the current ring design parameters are given in table 1. With

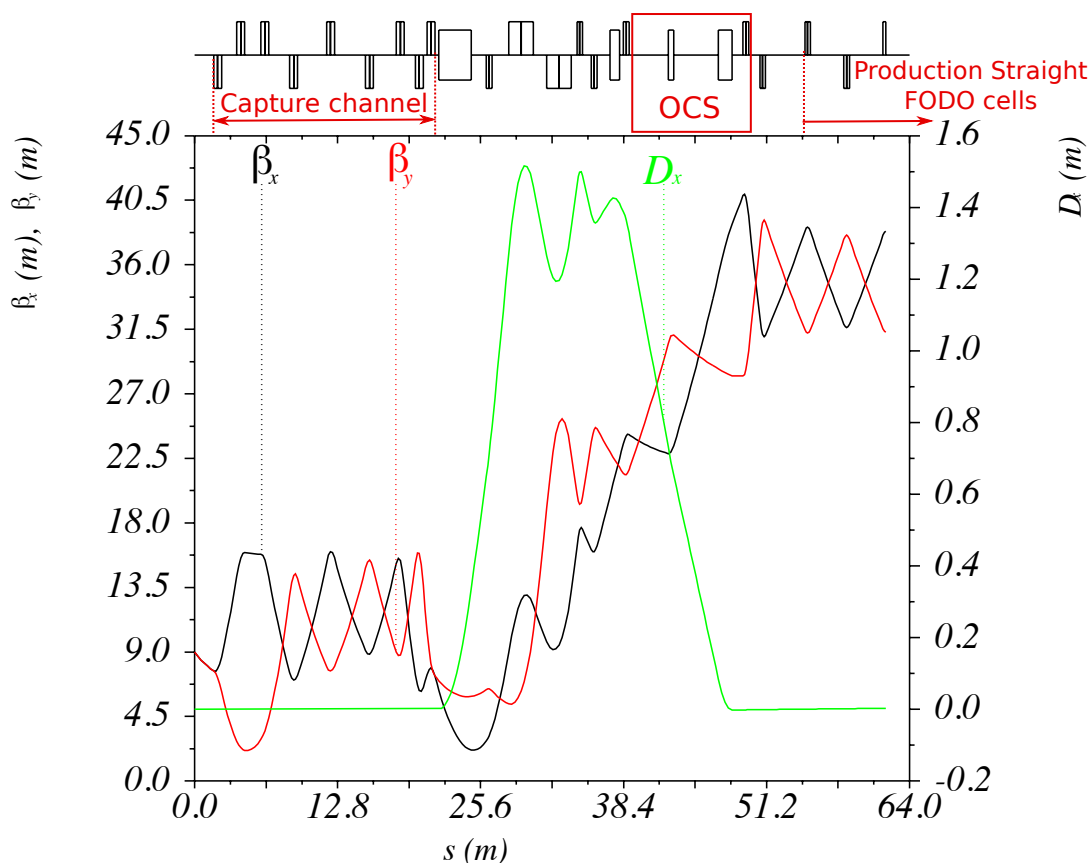


**Figure 4.** The linear optics of the pion beamline. The complete FODO production straight was replaced by a single FODO cell to avoid repeating periodic Twiss functions. The pions move from the left to the right in this figure.

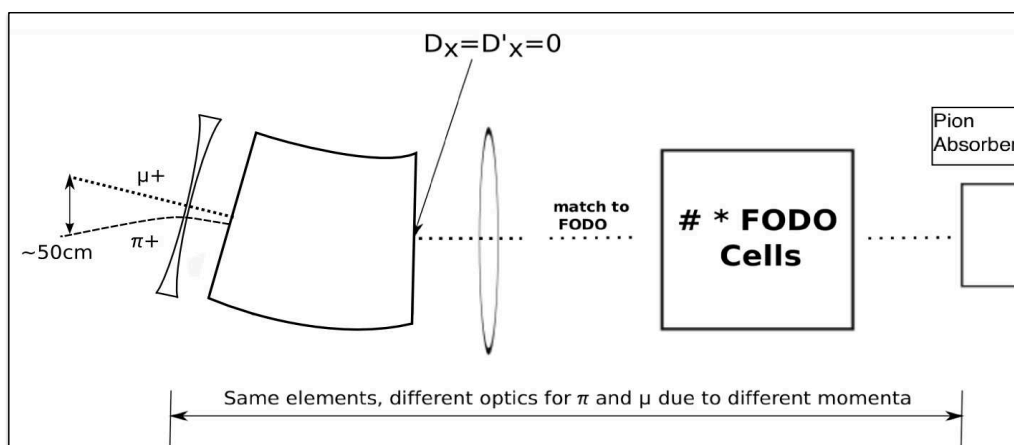


**Figure 5.** Schematic drawing of the orbit combination section (OCS). The green region indicated by the green vertical lines shows the  $3.8 \pm 10\%$  GeV/c acceptance of the ring, and the region indicated by the red lines shows the high momentum muons which will be extracted by the mirror OCS at the end of the injection straight.

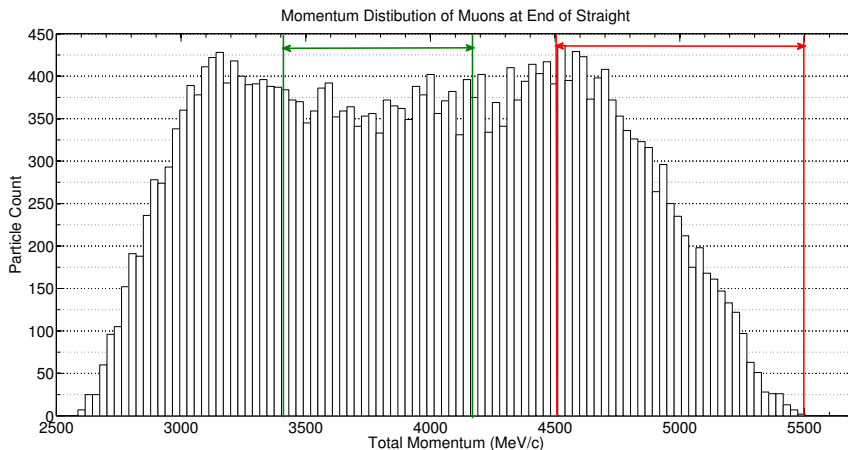


**Figure 6.** The muon momentum distribution at the end of decay straight.

the 185 m length for the injection straight,  $\sim 48\%$  of the pions decay before reaching the arc. Since the arcs are set for the central muon momentum of 3.8 GeV/c, the pions remaining at the end of the straight will not be transported by the arc, making it necessary to guide the remaining pion beam into an appropriate absorber. Another OCS, which is just a mirror reflection of the injection OCS, is placed at the end of the decay straight. It extracts the residual pions and muons that are in the  $5 \pm 0.5$  GeV/c momentum range. These extracted muons will enter the absorber along with pions in this same momentum band and can be used to produce an intense low-energy muon beam. With the lifetime of 3.8 GeV/c muons in the lab frame being  $\sim 79 \mu\text{s}$ , approximately 87% of them will decay (two lifetimes) in 100 turns. We define this 2 muon lab-frame lifetime as the useful store duration.



**Figure 7.** The decay ring layout. Pions are injected into the ring at the Orbit Combination section (OCS). Similarly, extraction of pions and muons at the end of the production straight is done using a mirror image of the OCS.

## 4 Performance

In this section we will give details on the neutrino beams that would be available at the nuSTORM facility. We show the observable event samples in a generic 100 ton and in a 1 kT SuperBIND detector (see section 4.2.1) located  $\approx 50$  m and 2 km, respectively, from the end of the production straight. Finally, we present a detailed discussion as to the physics reach in the neutrino oscillation  $\Delta m^2 - \sin^2 2\theta_{e\mu}$  phase space, assuming the detector described in section 4.2.1 at the 2 km position.

**Table 1.** Decay ring specifications.

Parameter	Specification	Unit
Central momentum $P_\mu$	3.8	GeV/c
Momentum acceptance	$\pm 10\%$	
Circumference	480	m
Straight length	185	m
Arc length	50	m
Arc cell type	DBA	
Ring Tunes ( $\nu_x, \nu_y$ )	9.72, 7.87	
Number of dipoles	16	
Number of quadrupoles	128	
Number of sextupoles	12	

#### 4.1 Neutrino fluxes and event samples

Uncertainty in the neutrino flux remains a significant source of systematic error for both neutrino interaction and oscillation experiments. The neutrino beams produced at nuSTORM can be determined with excellent precision with the use of conventional beam diagnostics tools to understand the parent particle distributions, from which the neutrino flux can then be precisely calculated. In order to determine the neutrino beams available at the nuSTORM facility, an ensemble of particles produced in a MARS [10] simulation of the target and horn were tracked using G4beamline [11], from the downstream face of the horn and then through the transfer line and injection into the decay ring via the OCS. The particles' energy and 4-momenta in the G4beamline tracking were then used to determine the neutrino flux at an arbitrary distance from the end of the production straight. This methodology was used to both determine the flux from the decay of circulating muons (those that decayed in the production straight) and from pions that decayed in the production straight. The calculation of the flux in this way presents a real-case flux determination based upon a modeled lattice and beam instrumentation. The errors on the binned flux are dependent solely on the knowledge of the particle trajectories and momentum distribution obtained by the beam diagnostics. In order to understand the effect of errors on the measurement of the beam divergence, simulations were conducted in which the beam divergence was inflated by 2% from nominal, chosen to encompass all possible sources of error. The flux at the detector location was calculated and compared to the flux produced by the nominal divergence. The bin-to-bin bias shown in figure 8 shows the error on the neutrino flux from a beam divergence error of 2%. The RMS error over the momentum range of 500 to 3500 MeV/c is 0.6%. A full description of the instrumentation proposed for nuSTORM can be found in [12].

A combination of instrumentation performance predictions and simulations indicate that the flux error will be below 1%. The simulated flux from the stored muon beam (for an exposure of  $10^{21}$  POT) is given in figure 9 (left) at the near detector position and in figure 9 (right) at the 2 km far detector position. The corresponding fluxes for pion decay are shown in figure 10. As can be seen in figure 10, nuSTORM produces an extremely pure  $\nu_\mu$  beam. Based on the flux calculations given above, the total number of neutrino interactions for a 100T detector at the 50m near position

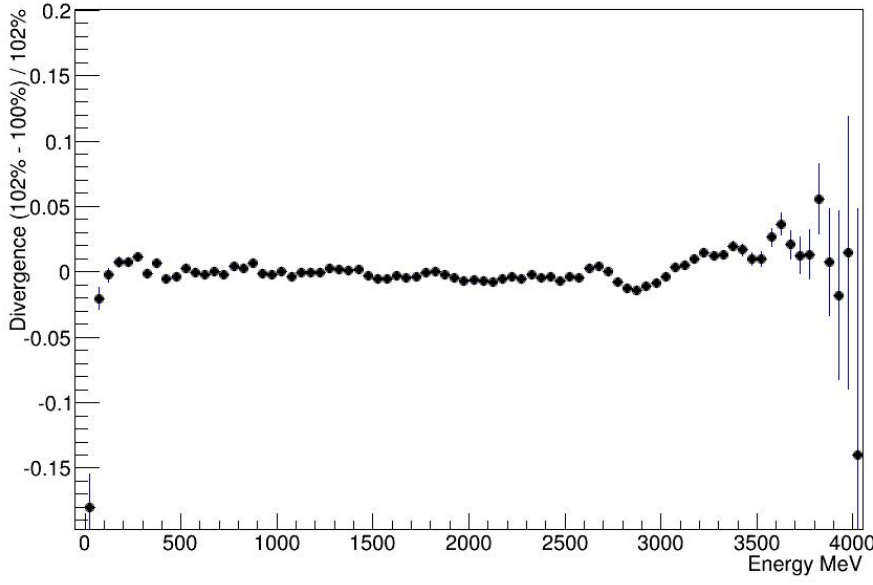


**Figure 8.** Bin-by-bin difference in neutrino flux with beam divergence inflated by 2% vs. nominal.

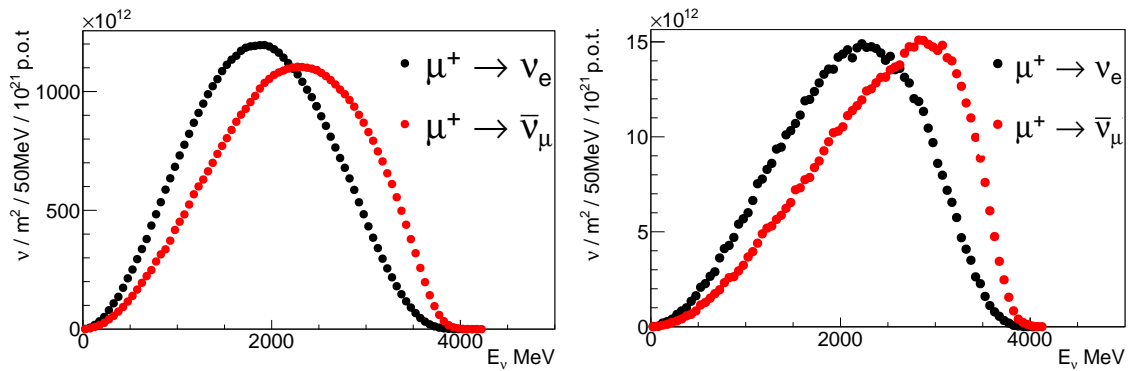


**Figure 9.** Neutrino flux from  $\mu$  decay at the near detector (left) and at the far detector (right).

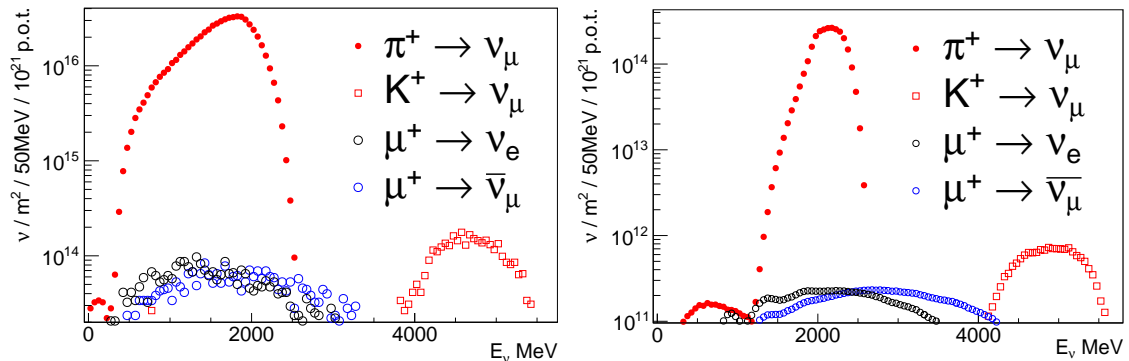


**Figure 10.** Neutrino flux from  $\pi$  decay at the near detector (left) and at the far detector (right). Events from  $K^+$  and  $\mu^+$  decay in the same transport and time window are also shown.

**Table 2.** Event sample at 50 m from the end of the decay straight per 100T for  $10^{21}$  POT.

$\mu^+$ Stored Channel	kEvents	$\mu^-$ Stored Channel	kEvents
$\nu_e$ CC	5,188	$\bar{\nu}_e$ CC	2,519
$\bar{\nu}_\mu$ CC	3,030	$\nu_\mu$ CC	6,060
$\nu_e$ NC	1,817	$\bar{\nu}_e$ NC	1,002
$\bar{\nu}_\mu$ NC	1,174	$\nu_\mu$ NC	2,074
$\pi^+$ Injected Channel	kEvents	$\pi^-$ Injected Channel	kEvents
$\nu_\mu$ CC	41,053	$\bar{\nu}_\mu$ CC	19,939
$\nu_\mu$ NC	14,384	$\bar{\nu}_\mu$ CC	6,986

**Table 3.** Event samples at 2 km per 1.3 kT for  $10^{21}$  POT for the no oscillation scenario and one with 1 sterile neutrino.

$\mu^+$ Stored		
Channel	No Oscillation	Oscillation
$\nu_e \rightarrow \nu_\mu$	0	288
$\nu_e \rightarrow \nu_e$	188,292	176,174
$\bar{\nu}_\mu \rightarrow \bar{\nu}_\mu$	99,893	94,776
$\bar{\nu}_\mu \rightarrow \bar{\nu}_e$	0	133
$\pi^+$ Injected		
Channel	No Oscillation	Oscillation
$\nu_\mu \rightarrow \nu_\mu$	915,337	854,052
$\nu_\mu \rightarrow \nu_e$	0	1,587

(exposure of  $10^{21}$  POT) can be determined and is shown in table 2. With a flux precision of  $\leq 1\%$  and with the statistics given in this table, nuSTORM offers unprecedented opportunities for the study of neutrino (both  $\bar{\nu}_\mu$  and  $\bar{\nu}_e$ ) interaction physics. Table 3 gives the number of events (again  $10^{21}$  POT) seen in a 1kT SuperBIND detector [13] at 2 km from the end of the production straight. The event samples, assuming no short-baseline oscillation and an oscillation scenario following a 3 + 1 scenario (3 standard neutrinos and 1 sterile neutrino), are both given in this table.

As can be seen in table 2 and table 3, nuSTORM simultaneously produces  $\bar{\nu}_\mu^+$  beams from  $\pi^\pm$  decay and  $\bar{\nu}_e^+$  and  $\bar{\nu}_\mu^+$  beams from  $\mu^\pm$  decay. These beams can support both a comprehensive neutrino scattering program at the near detector position and, at the far detector position, allow for the study of 6 oscillation channels. No other single facility can make this claim.

## 4.2 Search for light-sterile neutrinos

With an exposure of  $10^{21}$  120 GeV POT, the nuSTORM facility provides approximately  $1.9 \times 10^{18}$  useful  $\mu$  decays. The appearance of  $\nu_\mu$ , via the channel  $\nu_e \rightarrow \nu_\mu$ , gives nuSTORM broad sensitivity to sterile neutrinos and directly tests the LSND/MiniBooNE anomaly [14].

### 4.2.1 Far Detector

We have chosen an iron and scintillator sampling calorimeter (Super B Iron Neutrino Detector, SuperBIND) which is similar in concept to the MINOS detector [15]. It has a cross section of 6 m in order to maximize the ratio of the fiducial mass to total mass. The magnetic field will be toroidal, as in MINOS, and SuperBIND will also use extruded scintillator for the readout planes. However, SuperBIND will use superconducting transmission lines [16] to carry the excitation current and thus will provide a much larger B field in the steel ( $\approx 2$  T over most of the steel plate). Figure 11 gives an overall concept for the detector.

### 4.2.2 Results

A detailed detector simulation and reconstruction program has been developed to determine the detector response for the far detector in the short baseline experiment. Event reconstruction uses

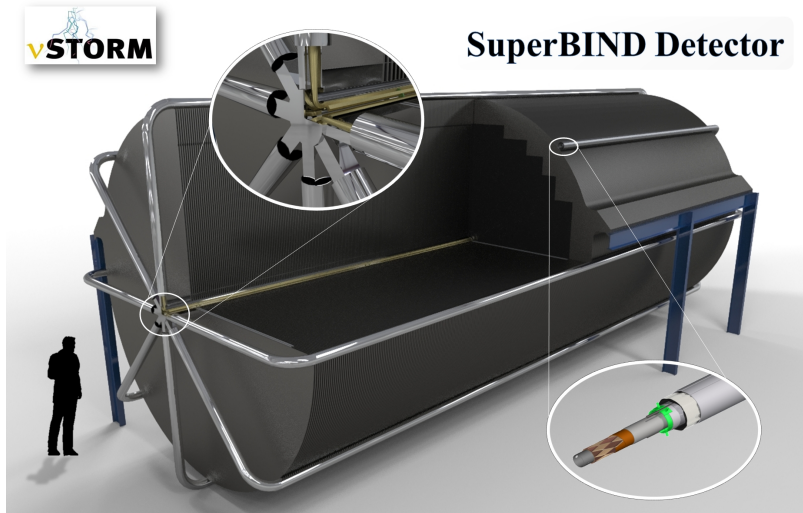


**Figure 11.** Far Detector concept. The insert in the upper left shows the 8 superconducting transmission lines combining in the central bore. The insert in the lower right shows a schematic of the superconducting transmission line.

multiple passes of a Kalman-filter algorithm to identify muon trajectories within events and to determine the momentum and charge of an identified track. Multiple tracks are identified within the simulation, and the length of all identified tracks is determined by a fitting algorithm. The longest track is chosen as the prospective muon track for the event and all other tracks are assumed to be the result of pion production or electron showers.

Following the reconstruction, the events are analyzed to select events with well reconstructed muon tracks, and to remove tracks that are mis-identified from pions or electron showers. The optimization of the muon neutrino appearance channel was conducted using the significance statistic  $S/\sqrt{S+B}$  where  $S$  is the total number of selected signal events and  $B$  is the number of background events selected. Several different multi-variate methods were tested for this analysis, but it was determined that the Boosted Decision Tree (BDT) method produced the best result [17]. The resultant integrated signal efficiency in this optimization is 0.17 with a background efficiency of  $4 \times 10^{-5}$ . This degree of background suppression is what allows for a measurement in this channel at the  $10\sigma$  sensitivity level. A contour plot showing the sensitivity of the  $\nu_\mu$  appearance experiment to sterile neutrinos, utilizing a boosted-decision-tree (BDT) multi-variate analysis, appears in figure 12 for the exposure given above. The 99% confidence level contours from a global fit to all experiments showing evidence for unknown signals (appearance + reactor + Gallium) and the contours derived from the accumulated data from all applicable neutrino appearance experiments [18] are also shown.

## 5 Optimization of the nuSTORM pion beam line for long-baseline oscillation physics

If the decay ring of nuSTORM is tilted, beams could be used for a long-baseline neutrino oscillation experiment. We have investigated this option, but have determined that the flux available from pion decay in the production straight is too small to be useful. We then considered a configuration that was optimized for the production of a  $\bar{\nu}_\mu$  beam from pion decay. We removed the capability

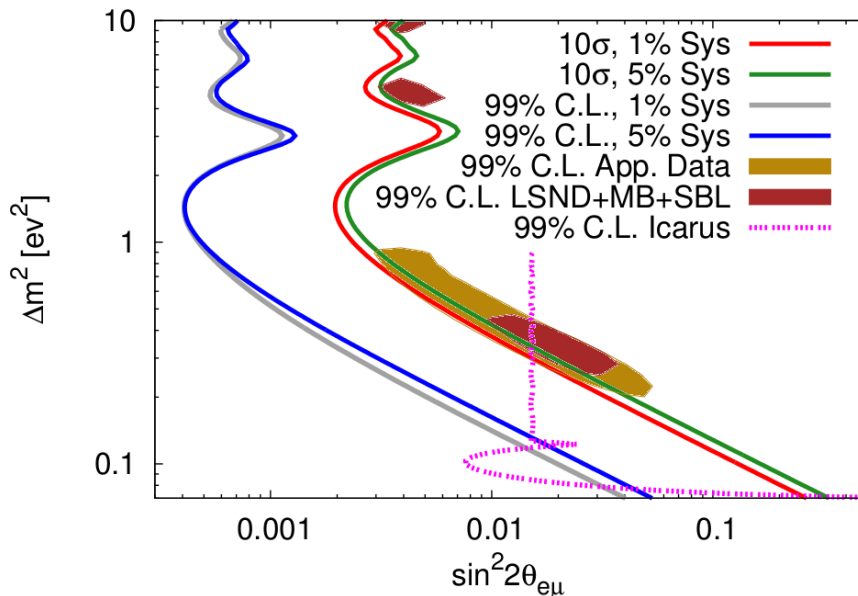


**Figure 12.** The sensitivity of a  $\nu_\mu$  appearance experiment to a short baseline oscillation due to a sterile neutrino at nuSTORM assuming a  $3 + 1$  model. Both the  $10\sigma$  significance and 99% confidence level contours are shown for two different scenarios for the systematic uncertainties; one in which the total systematic uncertainty is 1% of the beam normalization and a second when the systematic uncertainty is a factor of 5 times larger. The 99% contours generated from the fit to the MiniBooNE and LSND data are shown as the tan region, while the fit to all available appearance data is shown in brown (see [18]). The 99% exclusion contour from Icarus is also shown. [19]

for a stored muon beam, considering only a pion injection line (from the target to the end of the production straight). This concept of producing neutrinos from an instrumented pion beam line, nuPIL, is shown in figure 13. In this configuration, the injection OSC, the arcs and the return straight are removed (no ring) and the lattice design is only optimized to transport pions in a momentum band of  $5 \pm 1$  GeV/c. Since the straight is no longer required to transport both pions and muons (with a lower momentum), the compromises needed to do so are no longer incorporated and pion transport is more efficient. In this case, a simplified mirror OSC is used to extract the remaining pions (and some muons as described above) to a beam absorber. This pion injection beam line would, of course, need to be tilted at an appropriate angle.

Figure 14 shows the  $\nu_\mu$  flux/yr obtained at 1300 km for this configuration. This is for  $1.47 \times 10^{21}$  80 GeV POT. Also shown is the flux that would be obtained for nuSTORM and, for reference, the current baseline optimized flux for DUNE [20] (Optimized Beam, 80 GeV, 204 m  $\times$  4 m DP). The nuPIL flux uses an idealized target and a realistic (engineered) horn. The DUNE flux uses a realistic target and horn. This shows that this nuPIL configuration (FODO) produces  $\approx 40\times$  the flux of nuSTORM. The flux does fall short of what is obtained at DUNE, but the beam systematics will be greatly reduced since effects due to uncertainties in secondary particle production, proton-beam targeting stability, target degradation/stability and horn stability can be removed by in situ measurement of the pion flux (via beam line instrumentation) in the production straight. We plan to use a combination of fast beam-current transformers, beam position monitors and Direct Diode Detection Base-Band Q (3D-BBQ) for tune measurements. These are all in situ measurements. In

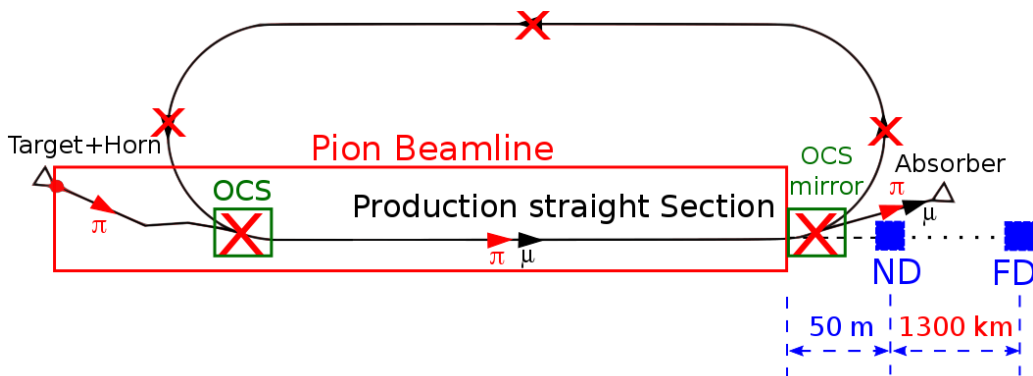


**Figure 13.** Schematic of the nuPIL pion injection line. The red Xs indicate the components removed from the nuSTORM configuration.

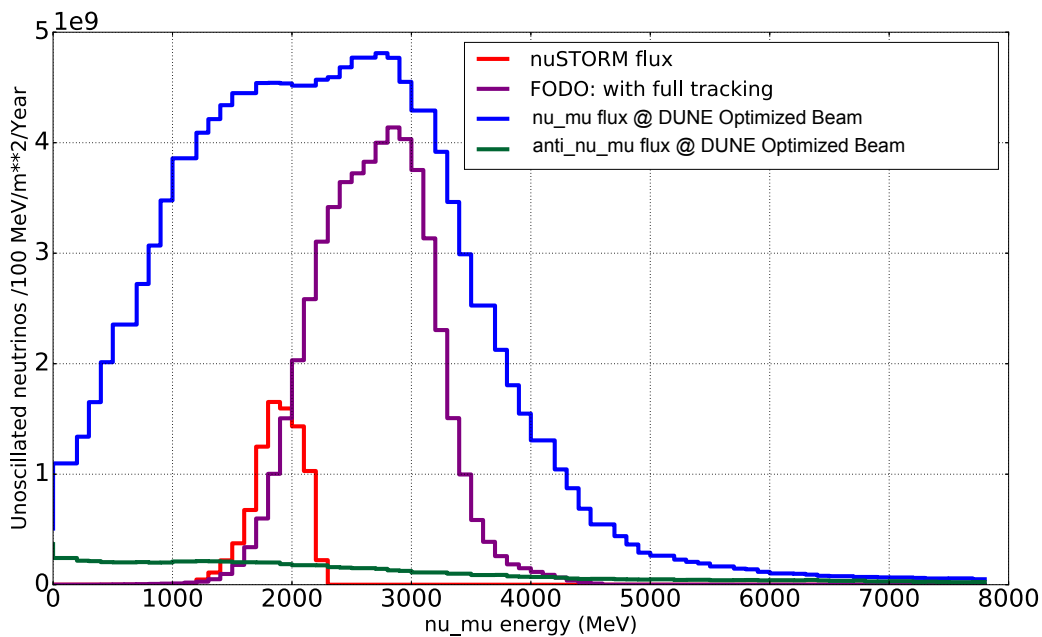


**Figure 14.** The neutrino flux ( $\nu_\mu$  from  $\pi^+$  decay at a distance of 1300 km) for nuSTORM and nuPIL. The flux for DUNE (Optimized Beam: 80 GeV, 204 m  $\times$  4 m DP [20]) is shown for comparison. In addition, the  $\bar{\nu}_\mu$  in the DUNE beam is also shown. For nuPIL, the  $\bar{\nu}_\mu$  contamination is negligible and is not visible on this plot.

addition, during calibration periods, destructive measurements can also be made in order to improve our understanding of the beam. See [12] for details. Furthermore, the wrong-flavor neutrinos ( $\nu_\mu$  in the  $\bar{\nu}_\mu$  beam and vice versa) and the high-energy component of the  $\bar{\nu}_\mu$  beams are essentially entirely suppressed in this neutrino beam line design.

## 5.1 nuPIL design based on the FFAG principle

In order to increase the flux, we developed several lattice designs utilizing Fixed-Field Alternating Gradient (FFAG) optics. The use of scaling FFAG magnets [21, 22] can substantially increase the momentum acceptance for the pion beam from the horn as compared to the FODO design. A schematic of the concept is shown in figure 15 and assumes that pions after the horn are transported in a 5.8 deg beam line arc consisting of large aperture FFAG magnets and then are either injected into a beam line production straight (composed of large bore quadrupoles or of straight scaling FFAG magnets [21]) or into a decay pipe. In this approach, the pions would go through a charge selection process in the bend, providing a cleaner neutrino beam at the detector. Furthermore, the engineering complexity of the beam line or the decay pipe is also lessened, since the remaining high energy protons would only be slightly bent. The remaining proton beam stays at surface level, which allows it to be directed to a relatively simple beam absorber. This simplifies the radiation safety issues in the production straight (beam line or decay pipe). Instrumentation can also be installed, as described above, giving the possibility to have access to an actual in situ measurement of the pion flux. Finally, the wrong sign pions could be extracted from the bending section and could be used to feed a nuSTORM facility running in parallel.

We developed many solutions, among which some used a dispersion creator followed by a dispersion suppressor. In this configuration, since dispersion will be matched to zero after the bend, the bend can be followed by a regular quad channel in the production straight section. In another configuration, with only a dispersion creator where dispersion would remain non-zero, the design used straight FFAG magnets in the straight. Both of these solutions could also assume decay pipe (no magnets in the production straight) and such a solution (called Lattice 11) is presented in this paper. It is a bending beam line composed of scaling FFAG magnets with a 5.8 deg bend and a decay pipe similar to the LBNF baseline scenario. The layout of the FFAG bend is presented in figure 16. First, a dispersion creator is used to adjust the dispersion (null after the horn) to a suitable value. Second, an optics matching section is used in order to minimize the divergence of the beam at the entrance of the decay pipe, while completing the required 5.8 degrees of bend. The dispersion is kept constant, while leaving zero derivative of dispersion at the end of the bend.

A pion distribution coming from a nuSTORM-like horn has been tracked in the FFAG bend. The momentum distribution of the pions at different points along the lattice (decays turned off) has been simulated and the results are presented in figure 17. The surviving particles have been used to compute the resulting neutrino flux and anti-neutrino flux at the far detector (see figures 18 and 19). We can see that the nuPIL concept has the potential to deliver a very pure neutrino beam for long-baseline neutrino experiments.

## 6 Conclusions

In this article we have summarized the status and capabilities of the nuSTORM facility. We have also shown how one component of the facility (the pion injection line) could be re-optimized solely for the production of  $\vec{\nu}_\mu$  from  $\pi^\pm$  decay, producing a neutrino beam with very small flux uncertainties and greatly reduced backgrounds.

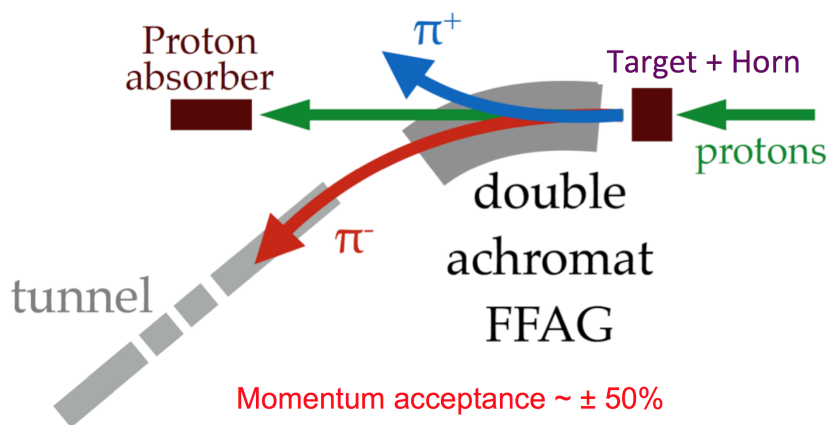


**Figure 15.** A schematic of the concept to extend the nuPIL design to a FFAG lattice.

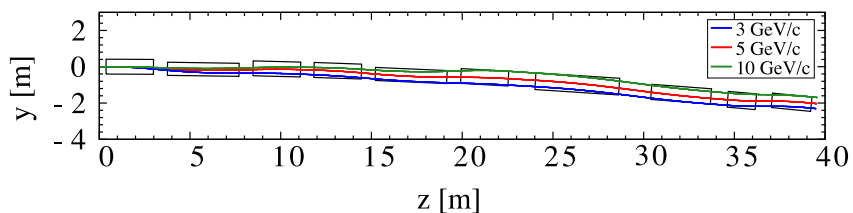


**Figure 16.** Layout of the nuPIL lattice 11 bend. The horn is at  $z = 0$ , and the decay pipe starts at  $z = 39$  m.

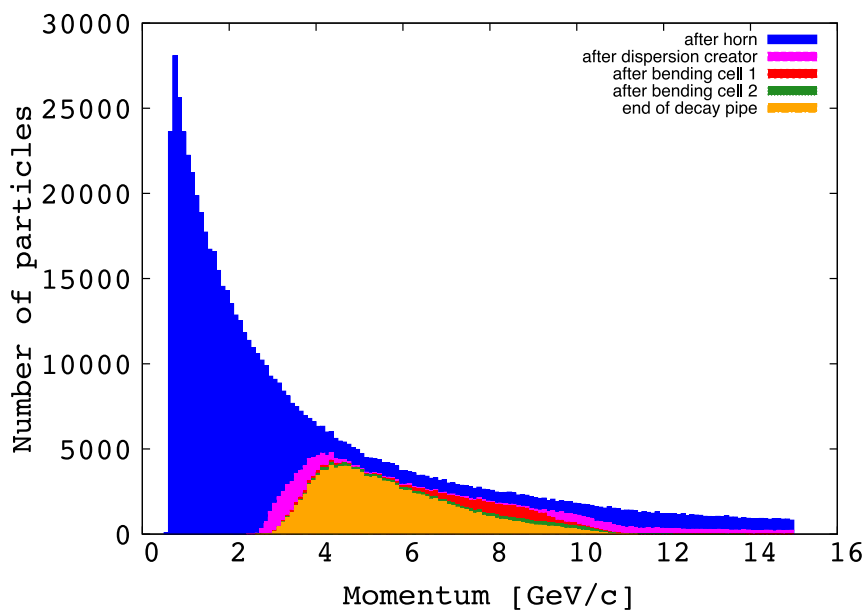


**Figure 17.** Momentum distribution of the pions from the nuSTORM horn at different places along lattice 11, with pion decay turned off in the simulation.

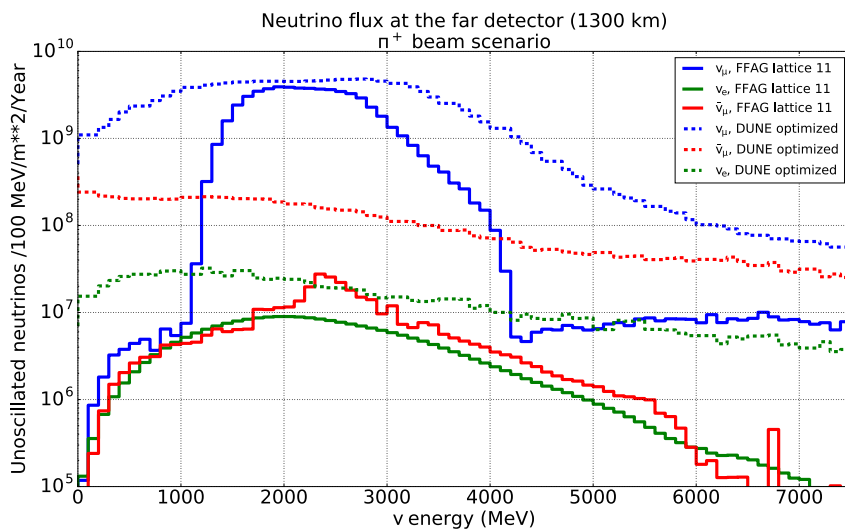


**Figure 18.** Neutrino flux at far detector with nuSTORM horn in nuPIL, lattice 11 (plain lines) and for the LBNF 2-horn optimized solution (dotted line).

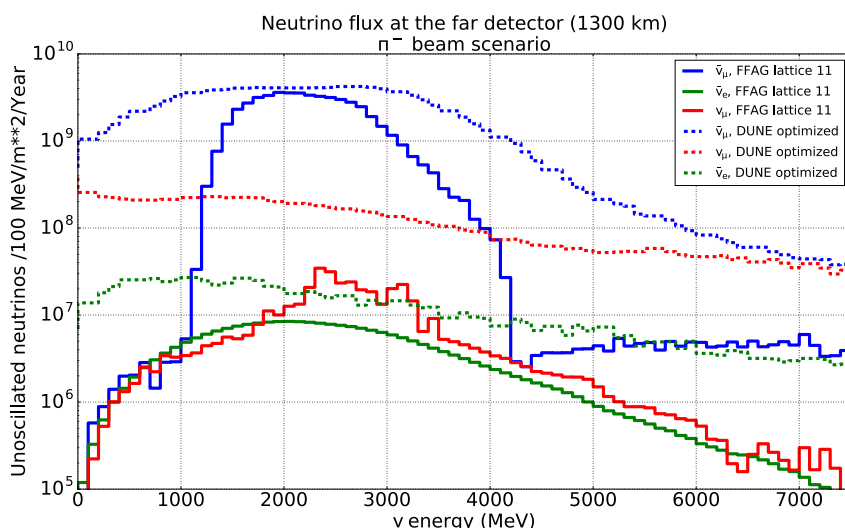


**Figure 19.** Anti-neutrino flux at far detector with nuSTORM horn in nuPIL, lattice 11 (plain lines) and for the LBNF 2-horn optimized solution (dotted line).

## Acknowledgments

We wish to thank Shyh-Yuan Lee, Laura Fields and Sergei Striganov for their valuable input to this study. In addition, we acknowledge the numerous contributions from our colleagues in the Muon Accelerator Program. Operated by Fermi Research Alliance, LLC under Contract No. DE-AC02-07CH11359 with the United States Department of Energy and the Science and Technology Facilities Council of the United Kingdom.

## References

- [1] nuSTORM collaboration, D. Adey et al., *nuSTORM - Neutrinos from STORed Muons: Proposal to the Fermilab PAC*, [arXiv:1308.6822](#).
- [2] D. Adey, R. Bayes, A. Bross and P. Snopok, *nuSTORM and A Path to a Muon Collider*, *Ann. Rev. Nucl. Part. Sci.* **65** (2015) 145.
- [3] S. Geer, *Neutrino beams from muon storage rings: Characteristics and physics potential*, *Phys. Rev. D* **57** (1998) 6989, [[hep-ph/9712290](#)].
- [4] THE IDS-NF collaboration, S. Choubey et al., *Interim Design Report for the International Design Study for a Neutrino Factory*, [arXiv:1112.2853](#).
- [5] T. Lackowski, S. Dixon, R. Jedziniak, M. Blewitt and L. Fink, *nuSTORM Project Definition Report*, [arXiv:1309.1389](#).
- [6] K. Anderson, B. Bernstein, D. Boehnlein, K.R. Bourkland, S. Childress et al., *The NuMI Facility Technical Design Report*, FERMILAB-DESIGN-1998-01, 1998.
- [7] D. Neuffer, *Design Considerations for a Muon Storage Ring Telmark*, in *Proceedings of Mini-Conference and Workshop on Neutrino Mass*, V. Barger and D. Cline eds., Telmark, Wisconsin, October 2–4 1980, pp. 199–203.
- [8] A. Liu, A. Bross, D. Neuffer and S. Y. Lee, *nuSTORM Pion Beamline Design Update*, in *Proceedings of the North American Particle Accelerator Conference*, Pasadena, CA, 29 September – 4 October 2013, pp. 562–564, [PAC-2013-TUPBA18].
- [9] A. Liu, D. Neuffer and A. Bross, *Design and Simulation of the nuSTORM Pion Beamline*, *Nucl. Instrum. Meth. A* **801** (2015) 44.
- [10] N. V. Mokhov, *Status of MARS code*, [arXiv:1409.0033](#).
- [11] T. Roberts, *G4beamline - A “Swiss Army Knife” for Geant4, optimized for simulating beamline*, <http://www.muonsinternal.com/muons3/G4beamline>, 2013.
- [12] L. Søby, *nuSTORM Beam instrumentation*, <https://edms.cern.ch/document/1284677/1>, 2013.
- [13] R. Bayes, A. Laing, F.J.P. Soler, A. Cervera Villanueva, J.J. Gomez Cadenas et al., *The Golden Channel at a Neutrino Factory revisited: improved sensitivities from a Magnetised Iron Neutrino Detector*, *Phys. Rev. D* **86** (2012) 093015, [[arXiv:1208.2735](#)].
- [14] E. Akhmedov and T. Schwetz, *MiniBooNE and LSND data: Non-standard neutrino interactions in a (3+1) scheme versus (3+2) oscillations*, *JHEP* **1010** (2010) 115, [[arXiv:1007.4171](#)].
- [15] MINOS collaboration, D.G. Michael et al., *The Magnetized steel and scintillator calorimeters of the MINOS experiment*, *Nucl. Instrum. Meth. A* **596** (2008) 190–228, [[arXiv:0805.3170](#)].
- [16] VLHC DESIGN STUDY GROUP collaboration, G. Ambrosio et al., *Design study for a staged very large hadron collider*, FERMILAB-TM-2149.
- [17] nuSTORM collaboration, D. Adey et al., *Light sterile neutrino sensitivity at the nuSTORM facility*, *Phys. Rev. D* **89** (2014) 071301, [[arXiv:1402.5250](#)].
- [18] J. Kopp, P.A.N. Machado, M. Maltoni and T. Schwetz, *Sterile Neutrino Oscillations: The Global Picture*, [arXiv:1303.3011](#).
- [19] ICARUS collaboration, M. Antonello et al., *Search for anomalies in the  $\nu_e$  appearance from a  $\nu_\mu$  beam*, *Eur. Phys. J. C* **73** (2013) 2599, [[arXiv:1307.4699](#)].

- [20] DUNE collaboration, *Fluxes used in for the 2015 CDR*, <http://home.fnal.gov/~ljf26/DUNE2015CDRFluxes/>, 2015.
- [21] J.B. Lagrange, T. Planche, E. Yamakawa, T. Uesugi, Y. Ishi, Y. Kuriyama et al., *Straight scaling FFAG beam line*, *Nucl. Instrum. Meth. A* **691** (2012) 55.
- [22] K. Symon, D. Kerst, L. Jones, L. Laslett and K. Terwilliger, *Fixed-Field Alternating-Gradient Particle Accelerators*, *Phys. Rev.* **103** (1956) 1837.

2017 JINST 12 P07020